Cerebral Cortex, 2018; 1–12

doi: 10.1093/cercor/bhy006
Original Article

ORIGINAL ARTICLE

Subthreshold Activity Underlying the Diversity and Selectivity of the Primary Auditory Cortex Studied by Intracellular Recordings in Awake Marmosets

Lixia Gao[1,2] and Xiaoqin Wang[1]

[1]Laboratory of Auditory Neurophysiology, Department of Biomedical Engineering, Johns Hopkins University School of Medicine, Baltimore, MD 21205, USA and [2]Interdisciplinary Institute of Neuroscience and Technology, Qiushi Academy for Advanced Studies, Zhejiang University, Hangzhou 310029, People's Republic of China

Address correspondence to Xiaoqin Wang, Department of Biomedical Engineering, Johns Hopkins University School of Medicine, 720 Rutland Ave., Traylor 410, Baltimore, MD 21025, USA. Email: xiaoqin.wang@jhu.edu; Lixia Gao, Interdisciplinary Institute of Neuroscience and Technology, Qiushi Academy for Advanced Studies, Zhejiang University, 268 Kaixuan Road, Science Building, Room 206, Hangzhou, Zhejiang 310029, China. Email: lxgao10@zju.edu.cn

Abstract

Extracellular recording studies have revealed diverse and selective neural responses in the primary auditory cortex (A1) of awake animals. However, we have limited knowledge on subthreshold events that give rise to these responses, especially in non-human primates, as intracellular recordings in awake animals pose substantial technical challenges. We developed a novel intracellular recording technique in awake marmosets to systematically study subthreshold activity of A1 neurons that underlies their diverse and selective spiking responses. Our findings showed that in contrast to predominantly transient depolarization observed in A1 of anesthetized animals, both transient and sustained depolarization (during or beyond the stimulus period) were observed. Comparing with spiking responses, subthreshold responses were often longer lasting in duration and more broadly tuned in frequency, and showed narrower intensity tuning in non-monotonic neurons and lower response threshold in monotonic neurons. These observations demonstrated the enhancement of stimulus selectivity from subthreshold to spiking responses in individual A1 neurons. Furthermore, A1 neurons classified as regular- or fast-spiking subpopulation based on their spike shapes exhibited distinct response properties in frequency and intensity domains. These findings provide valuable insights into cortical integration and transformation of auditory information at the cellular level in auditory cortex of awake non-human primates.

Key words: auditory cortex, intracellular recording, marmoset, regular- and fast-spiking neurons, stimulus selectivity

Introduction

Extracellular recording studies of the primary auditory cortex (A1) have revealed diverse and selective neural responses (Schreiner et al. 2000; Nelken 2008; Wang et al. 2008). However, the subthreshold mechanisms underlying neural diversity and selectivity in A1 of awake animals have remained largely unknown, as intracellular recording in awake animals poses substantial technical challenges, especially in non-human primates. A number of studies have shown that neural responses in sensory cortex of awake animals differ in many aspects from those observed in anesthetized animals (Matsumura et al. 1988; Lu and Wang 2000; Wang et al. 2005, 2008; Ter-Mikaelian et al. 2007; Qin et al. 2008; Long et al. 2010; Sadagopan and Wang 2010; Bartlett et al. 2011; Constantinople and Bruno 2011;

Long and Lee 2012; Haider et al. 2013; Gao and Wehr 2015). In anesthetized animals of various species, neurons in the primary auditory cortex (A1) generally showed transient response (onset and/or offset) regardless the length of sound duration (Phillips 1985; Heil 1997; DeWeese et al. 2003; Wehr and Zador 2003; Zhang et al. 2003; Wu et al. 2008; Zhou et al. 2010) and most commonly monotonic rate-level functions (Schreiner et al. 1992; Phillips et al. 1995; Wu et al. 2006, 2008; Li et al. 2014). In contrast, A1 neurons in awake animals exhibit a greater variety of temporal response patterns including both onset/offset and sustained firings in response to acoustic stimulation (Brugge and Merzenich 1973; Bieser and Muller-Preuss 1996; Lu et al. 2001a, 2001b; Liang et al. 2002; Malone et al. 2002; Wang et al. 2005; Bendor and Wang 2007; Hromadka et al. 2008; Qin et al. 2008; Chambers et al. 2014; Gao and Wehr 2015; Gao et al. 2016); a greater proportion of non-monotonic responses (Pfingst and O'Connor 1981; Sadagopan and Wang 2008, 2010; Watkins and Barbour 2011). Thus far, cellular mechanisms responsible for response diversity and selectivity in A1 have been studied mainly in anesthetized animals (Wehr and Zador 2003; Zhang et al. 2003; Tan et al. 2004, 2007; Wu et al. 2006, 2008, 2011; Li et al. 2013, 2014, 2015; Zhou et al. 2014; Mesik et al. 2015). We have little knowledge on how such mechanisms may operate in A1 of awake animals. Given the state dependency of A1 demonstrated in previous studies (Romo and Salinas 2003; Polley et al. 2004; Fritz et al. 2007, 2010; Issa and Wang 2008; Niell and Stryker 2010; Polack et al. 2013; Zhou et al. 2014; McGinley, David, et al. 2015), it is important to examine subthreshold responses in awake animals.

There has been a growing number of intracellular recording studies in awake animals, primarily in rodents (Steriade et al. 2001; Kitano et al. 2002; Lee et al. 2006, 2009, 2014; Poulet and Petersen 2008; Niell and Stryker 2010; Okun et al. 2010; Long and Lee 2012; Haider et al. 2013; Tan et al. 2014; Zhou et al. 2014; McGinley, David, et al. 2015). However, intracellular recordings in non-human primates especially in awake conditions have been rare because of considerable technical challenges due to large mechanical disturbances related to animals' heart beat and breathing (Lee et al. 2009, 2014; Long and Lee 2012). We have developed a novel intracellular recording technique that allows us to repeatedly and reliably record both spiking responses and membrane potentials (MP) from a relatively large number of neurons in a single marmoset under awake condition. Marmosets are a highly vocal and social non-human primate species with a similar hearing range as humans (Agamaite et al. 2015; Miller et al. 2016; Osmanski and Wang 2011). Auditory cortical neurons in awake animals show a high degree of response diversity and selectivity. However, the underlying cellular mechanisms remain mostly unclear. In the present study, we focused on evaluating subthreshold responses that contribute to the diversity and selectivity of A1 neurons in awake marmosets in frequency and intensity domains. Our results showed the enhancement of stimulus selectivity from subthreshold responses to spiking responses in individual A1 neurons. Moreover, we found distinct response properties of regular- from fast-spiking neurons in frequency and intensity domains. These results obtained from A1 of awake marmosets provide valuable insights into cortical processing of acoustic information at the cellular level in non-human primates. The intracellular recording technique developed in our study opens the door for further studies of cellular mechanisms underlying complex and natural sound processing in population of neurons in auditory cortex of marmosets or other animal models (Wang 2000; Mizrahi et al. 2014).

Materials and Methods

Animal Preparation

Experiments were conducted in awake marmosets (*Callithrix jacchus*) with both male and female sexes. Auditory brainstem response was measured to confirm that the animals had normal hearing. The animals were trained to sit quietly in a custom-designed primate chair. After 2–4 weeks of chair-adaptation, 2 stainless steel head-posts were attached to the skull with dental cement under sterile conditions under isoflurane anesthesia (0.5–2.0%, mixed with 50% oxygen and 50% nitrous oxide). The skull over auditory cortex was exposed and covered with a thin layer of dental cement and a wall around the recording chamber was molded from the same material. After the animal fully recovered from the head-post implant surgery (usually 3–4 weeks), a miniature craniotomy (⌀ ~ 1 mm) was made over the superior temporal gyrus to allow the electrodes to access the auditory cortex. The top half of the craniotomy was enlarged (⌀ ~ 2 mm) to increase the space for the electrode manipulation. Several daily recording sessions were made through each recording hole. At the end of each recording session, the recording hole was thoroughly rinsed with sterile saline and filled with a silicone plug to prevent contamination and suppress tissue growth. Typically, 5–10 electrode penetrations were made within each recording hole over several recording sessions, after which the hole was permanently sealed with dental cement, and another craniotomy was made for new electrode penetrations. The above procedures were similar to the methods used in extracellular recordings and intracellular recordings from awake marmosets as described in previous publications from our laboratory (Lu et al. 2001a, 2001b; Wang et al. 2005; Gao et al. 2016).

Intracellular Recording Procedures

These procedures were identical to those described in previous publications from our laboratory (Gao et al. 2016). Intracellular recordings were made in the superficial layers (300–1200 μm) of A1 through the intact dura using a concentric sharp electrode and guide tube assembly (see Fig. 1 of Gao et al. 2016). This technique allowed us to perform intracellular recordings repeatedly in a single animal over many sessions and obtain a much larger number of neurons than permitted by traditional intracellular recording techniques commonly used in rodents. In brief, the location of A1 was determined by its tonotopic organization (caudal-medial: high frequency to low frequency), best frequency (BF) reversals at the rostral and caudal ends, its relationship to the lateral belt area (which was more responsive to noises than tones), and its response properties (e.g., more responsive to tonal stimuli) as described in our laboratory's previous publications on the awake marmoset (Lu et al. 2001a, 2001b; Bendor and Wang 2007). The recording pipette was made of quartz glass (QF100-50-10, ID = 0.5 mm, OD = 1.0 mm, Sutter Instrument) rather than the traditional borosilicate glass to improve the strength of recording electrodes in order to penetrate through the intact dura. This allowed us to record over 5–7 sessions in a single craniotomy with minimal damage to the cortex (a new pipette was used for each penetration). The recording pipette was pulled by a laser puller (P-2000, Sutter Instrument) to a resistance of 90–120 MΩ and back-filled with

3.0 M KAc (pH 7.6, Sigma). We used a co-axial guide tube made of borosilicate glass pipette (B150-110-7.5, ID = 1.1 mm, OD = 1.5 mm, Sutter Instrument) concentric to the recording electrode to provide protection for the sharp electrode tip, both of which were fastened into a custom-made electrode holder. The electrode assembly was advanced perpendicularly relative to the brain surface with a motorized manipulator (DMA1510, Narishige). Once the initial recording depth was reached (300–400 μm below the dura), the recording electrode was manually decoupled from the guide tube which was temporarily fixed into the recording chamber with dental impression material (EXAMIX™ NDS, Kerr Dental). At this point, the recording electrode can move independently of the guide tube and was advanced into the cortex. The recording electrode was lowered at 4 μm steps. If the sharp electrode penetrated the cell membrane, the voltage recorded would drop to negative value. Considering the leakage after electrode penetration, we usually collected data at least 1 min after the MP dropped. Our criteria for high quality recordings is that the rest MP is below −50 mV and the amplitude of spike is larger than 50 mV. After the micropipette was stabilized for a few minutes inside the cell and the voltage stayed below −50 mV, we commenced to present auditory stimuli while recording both the spikes and the MP dynamics. The electrical signals were amplified using Axoclamp 2B (Molecular Devices), digitized (RX6, Tucker-Davis Technologies), analyzed and saved using custom programs written in Matlab (Mathworks). Each daily recording session lasted 4–5 h. All recording sessions were conducted within a double-walled soundproof chamber (Industrial Acoustics). The interior of the chamber was covered by 3 inches acoustic absorption foam (Sonex).

Acoustic Stimuli

Acoustic signals were generated digitally in Matlab (MathWorks) at a sampling rate of 97.7 kHz with custom software, converted to analog signals (RX6, Tucker-Davies Technologies), power amplified (D75A, Crown Audio), attenuated (PA5, Tucker-Davies Technologies), and delivered in free-field through a loudspeaker (600S3, B&W) located approximately 1 m in front of the animal. Once a neuron was held, frequency tuning curve was determined by playing pure tones 100 ms in duration with 5 ms cosine ramps which spanned 3–4 octaves around a manually determined center frequency in 0.1-octave steps. The BF of a neuron was defined as the centroid of the frequency tuning curve at 40 dB SPL. Rate-level function of the recorded neuron was determined by varying the sound intensity which ranged from −10 to 80 dB in 10 dB steps. The best level (BL) of a neuron was defined as the sound level that elicited the maximal firing rate at BF.

Data Analysis

Neuronal signals were continuously digitized and saved onto a computer during each stimulus presentation including prestimulus and poststimulus windows. Both the MP and spike data were analyzed offline using custom software implemented in Matlab (Mathworks). Spikes were detected online by setting a threshold of at least 30 mV above the baseline of the MP. The spiking activities analysis methods used were the same as in our previous publications (Bendor and Wang 2008; Sadagopan and Wang 2008). In brief, average discharge rates were calculated over the entire stimulus duration and the mean spontaneous rate (estimated over the entire stimulus set) was subtracted in all analyses. The criterion for a significant stimulus-driven spiking response was defined as an averaged discharge rate 2 standard deviations (SDs) above the mean spontaneous discharge rate. To obtain the subthreshold response, action potentials were removed from intracellular recording signal by line interpolation as described in previous paper (Zanos et al. 2011). The baseline of the MP was defined by the mean value of MP in an analysis window of 50 ms with minimal fluctuations by sliding the analysis window at every 10 ms step throughout the prestimulus duration. The magnitude of subthreshold response was defined by the area of depolarization or hyperpolarization over the stimulus duration. The spontaneous subthreshold response was defined by the mean area of MP fluctuations before sound presentation over the entire stimulus set. The criteria for a significant subthreshold response were defined as an averaged subthreshold area 2*SDs above the spontaneous subthreshold response.

The tuning bandwidth (in octaves) of A1 neurons was taken as the width at half maximum firing rate or the subthreshold response after we plotted the frequency tuning curve at BL or 40 dB SPL in 0.1-octave steps. The firing rate or subthreshold response at each tone was computed over the entire response duration. A monotonicity index (MI) was defined as the ratio of the mean discharge rate at the highest sound level tested (HL, typically 80 dB SPL) to the mean discharge rate at the neuron's BL. The mean spontaneous firing rate was subtracted from the calculation of mean discharge rate in this analysis. Neurons with a MI greater than 0.75 were defined as monotonic neurons, whereas neurons with MI less than or equal to 0.75 were defined as non-monotonic neurons (Bendor and Wang 2008). We calculated MI of the subthreshold response as well, which was defined as the ratio of the mean subthreshold response at HL to that at BL. The mean spontaneous MP fluctuation was subtracted from the calculation of the mean subthreshold response in this analysis. The response threshold of the spiking and subthreshold response was defined by the lowest sound level that was able to elicit significant stimulus-driven spiking/subthreshold responses. Threshold values were measured at each neuron's BF by varying stimulus level.

Classification of A1 neurons into regular-spiking (RS) and fast-spiking (FS) neurons was based on 2 features of the spike shape, spike width and slope of after-hyperpolarized-potential (AHP), using the method established in previous studies (McCormick et al. 1985; Steriade et al. 2001; Nowak et al. 2003; Cardin et al. 2007; Wu et al. 2008; Subkhankulova et al. 2010; Lewis et al. 2012; Li et al. 2014). Intracellularly recorded neurons with spike amplitude larger than 40 mV and stable spike waveform were used in this analysis. Spike width of individual A1 neurons was defined as the mean width of action potential at the half-amplitude of maximal. The slope of AHP was defined as the slope of the linear fit of membrane potential in 2 ms analysis window starting from the time point with minimum MP. Using these 2 features, we categorized A1 neurons into RS and FS neurons. FS neurons were defined as the neurons with narrow spikes (<0.3 ms) and pronounced AHP, whereas RS neurons were defined as the neurons with broad spikes (≥0.3 ms) and small or none AHP.

Results

Data presented in this study are based on a total of 106 intracellularly recorded neurons from A1 of 5 hemispheres in 4 awake marmosets (1 male, 3 females). Because of the limited recording time, not all stimulus paradigms were tested in each neuron. For each stimulus paradigm, a subset of 106 neurons were tested.

Temporal Response Patterns Evoked by Pure Tones

We studied intracellular responses to pure tones at various frequency and intensity in 55 A1 neurons. A1 neurons exhibited diverse temporal response patterns to pure tone stimuli in both subthreshold and spiking activity, showing both sustained and transient responses as shown by three example neurons in Figure 1A–C. Sustained firing was usually observed in response to tones at or close to a neuron's BF whereas onset-only responses were typically observed for tones away from BF (Fig. 1A–C, right). Mirroring sustained firing to tones at BF, we observed sustained subthreshold depolarization throughout the entire stimulus duration (Fig. 1A–C, left). The amplitude and duration of sustained depolarization decreased as the stimulus frequency deviated away from BF. In many cases, subthreshold responses lasted longer than spiking activities (Fig. 1G–I). Only a few neurons recorded in A1 of awake marmosets exhibited solely onset subthreshold and spiking responses to pure tone stimulation, which were typically observed in A1 of anesthetized animals (Phillips 1985; Heil 1997; DeWeese et al. 2003). The temporal response patterns of A1 neurons could be further modified from pure tone responses if more complex and preferred stimuli were used (Wang et al. 2005). However, our ability to identify the preferred stimulus of each neuron was much more limited in intracellular recordings. The prominence of sustained firing and subthreshold depolarization observed in A1 of awake marmosets suggest that anesthesia may profoundly reduce the sustained synaptic inputs to A1 neurons, consequently reducing the diversity of temporal responses.

Enhancement of Frequency Selectivity from Subthreshold to Spiking Response

BFs of A1 neurons measured by subthreshold responses were consistent with those measured by spiking responses (Fig. 1D–F). However, the frequency tuning measured by spiking responses was sharper than that measured by the subthreshold responses from the same neuron (Fig. 1D–F). In 55 A1 neurons studied

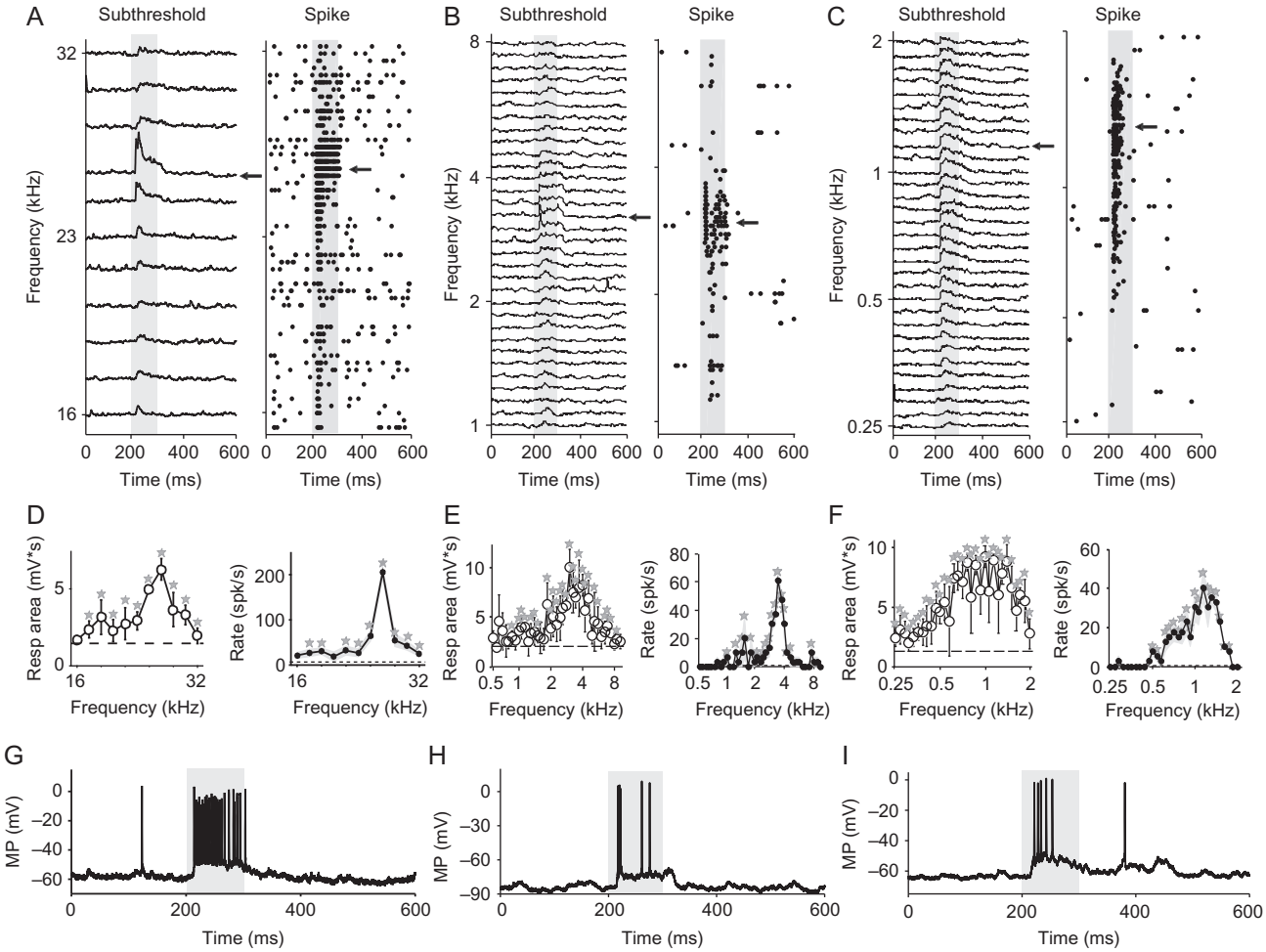

Figure 1. Frequency tuning properties of A1 neurons in awake state. *A*, *B*, *C*, Examples of subthreshold and spiking responses elicited by pure tones from three representative A1 neurons (M80Z0114, M22W0656, M14U1076). The spike width is 0.71, 0.25, and 0.71 ms, respectively. *Left*, mean subthreshold responses of 5 repetitions at each frequency. *Right*, raster plots of corresponding spiking responses. Gray shaded area indicates the duration of pure tone stimuli. Arrows points to the response to BFs of these 3 neurons. *D*, *E*, *F*, Frequency tuning curves measured by subthreshold response magnitude (left) and firing rate (right), respectively, averaged over the duration of the pure tone stimuli across 5 trials for the three example neurons shown in *A*–*C*. Error bars and the gray area represent standard deviation. Dashed horizontal lines indicate mean spontaneous subthreshold response (left) or mean spontaneous firing rate (right) of each neuron. Asterisks indicate evoked responses that are significantly different from spontaneous responses. *G*, *H*, *I*, Example intracellular recording traces showing responses to BF tones for the three example neurons shown in *A*–*C*, respectively. Gray shaded area indicates the duration of pure tone stimuli.

with pure tones, we calculated frequency tuning bandwidths of spiking and subthreshold responses as shown in Figure 2A, B, respectively. For the majority of neurons, tuning bandwidth of the spiking response was narrower than that of the subthreshold response (Fig. 2C). This may be due to the "iceberg effect" suggested in the primary visual cortex, narrowed orientation tuning from subthreshold to spiking response due to modulation of spiking threshold (Vidyasagar et al. 1996). The distribution of frequency tuning bandwidths measured by spiking response as shown in Figure 2A is consistent with that reported in previous extracellular recording studies in A1 of awake marmosets (Bartlett et al. 2011) and is substantially sharper than that observed in anesthetized marmosets (Kajikawa et al. 2005). Out of 55 neurons recorded from awake marmosets in the present study, 39 neurons had frequency tuning bandwidth of spiking responses smaller than 0.5 octaves. In contrast, only 5/38 sites showed frequency tuning bandwidth smaller than 0.5 octave measured at 10 dB above threshold in anesthetized marmosets by Kajikawa et al. (2005). These results suggest that under awake conditions A1 neurons may receive stronger intracortical inhibitory modulation that sharpens frequency tuning or inherit narrower frequency tuning from subcortical inputs. Another possibility is that the "iceberg effect" could be stronger in awake animals than in anesthetized animals.

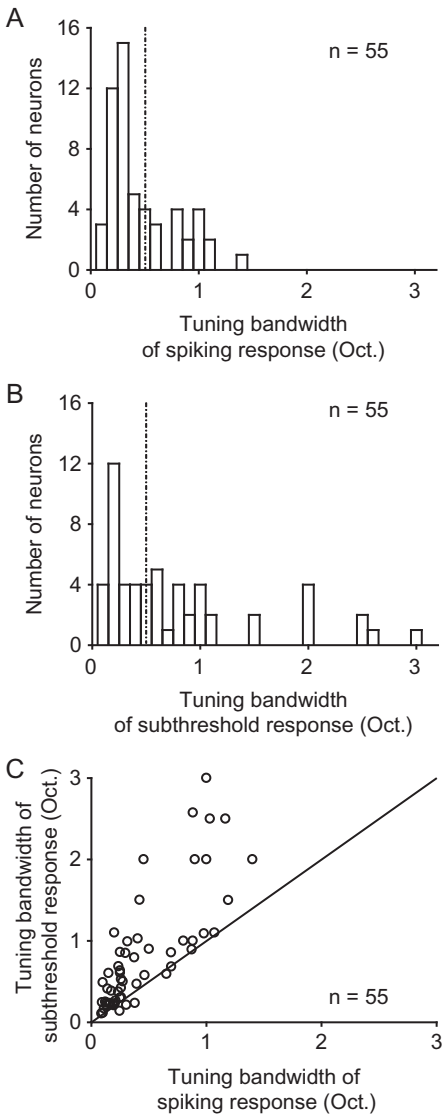

Figure 2. Tuning bandwidth of subthreshold and spiking responses in A1 neurons. A, B, Distributions of tuning bandwidths of spiking (A) and subthreshold (B) responses for all A1 neurons (n = 55). Vertical dashed line marks bandwidth of 0.5 octaves. Bin of width is 0.1 octaves. C, Tuning bandwidth of subthreshold response is plotted against that of spiking response for the same population of neurons as shown in A and B.

Subthreshold Mechanisms Underlying Sound Intensity Tuning

Based on spiking responses, rate-level functions of A1 neurons were classified as monotonic or non-monotonic (e.g., Sadagopan and Wang 2008). Previous studies have proposed models to explain the synaptic mechanisms underlying monotonic and non-monotonic rate-level functions in the auditory cortex (Ojima and Murakami 2002; Wu et al. 2006; Tan et al. 2007; de la Rocha et al. 2008). However, few were based on data obtained from awake animals. To elucidate these mechanisms in awake marmosets, we recorded intracellular responses to BF tone stimuli at different sound levels in 65 A1 neurons. About 50% of the sampled neurons (n = 33) exhibited monotonic rate-level functions in their spiking responses (MI > 0.75, see Methods) where firing rate increased with increasing sound intensity (Fig. 3A, D, right). The rest of neurons (n = 32, Fig. 4A) showed non-monotonic rate-level functions in their spiking responses (MI < 0.75, see Methods) with the peak firing rate reached at an intermediate sound level (Fig. 3B, C, E, F, right). When subthreshold responses were examined, monotonic neurons showed increased amplitude in depolarization with increasing sound level and the largest depolarization at the highest sound level tested (Fig. 3A, left). The depolarization in monotonic neurons typically lasted over the entire stimulus duration and often beyond as shown by the example in Figure 3A (left) and Figure 3G. Although the amplitudes of both spiking and subthreshold responses in monotonic neurons increased with sound level, the response threshold was much lower in subthreshold response than in spiking response as shown by the example neuron in Figure 3D and population analysis in Figure 4B, suggesting a transformation from subthreshold response to spiking response on the sound level threshold in monotonic neurons.

A1 neurons that exhibited non-monotonic rate-level functions can be divided into 2 subtypes. The majority (25/32 neurons) showed only depolarized subthreshold responses where the largest depolarization was found at moderate sound levels rather than at the highest sound level tested (Fig. 3B, E, left). These non-monotonic neurons typically exhibited weak depolarization at the highest sound level that failed to reach the spike threshold (Fig. 3B, E, H). A small proportion of the non-monotonic neurons (7/32) exhibited hyperpolarization instead of weak depolarization at the highest sound level tested, which resulted in suppressed firing in neurons with high spontaneous firing rates (Fig. 3C, F, I). This was also reflected by the negative value of the MI of the spiking response of these neurons (Fig. 4C). For the majority of non-monotonic neurons, the MI of the spiking response was smaller than the MI of the subthreshold response (Fig. 4C), which suggests an increase in non-monotonicity of the rate-level function of A1 neurons in awake marmosets. Figure 4C also shows that a subset of the non-monotonic neurons has the MI of the subthreshold response approaching 1.0 (i.e., being monotonic), which suggests that the non-monotonicity observed in A1 neurons is not entirely

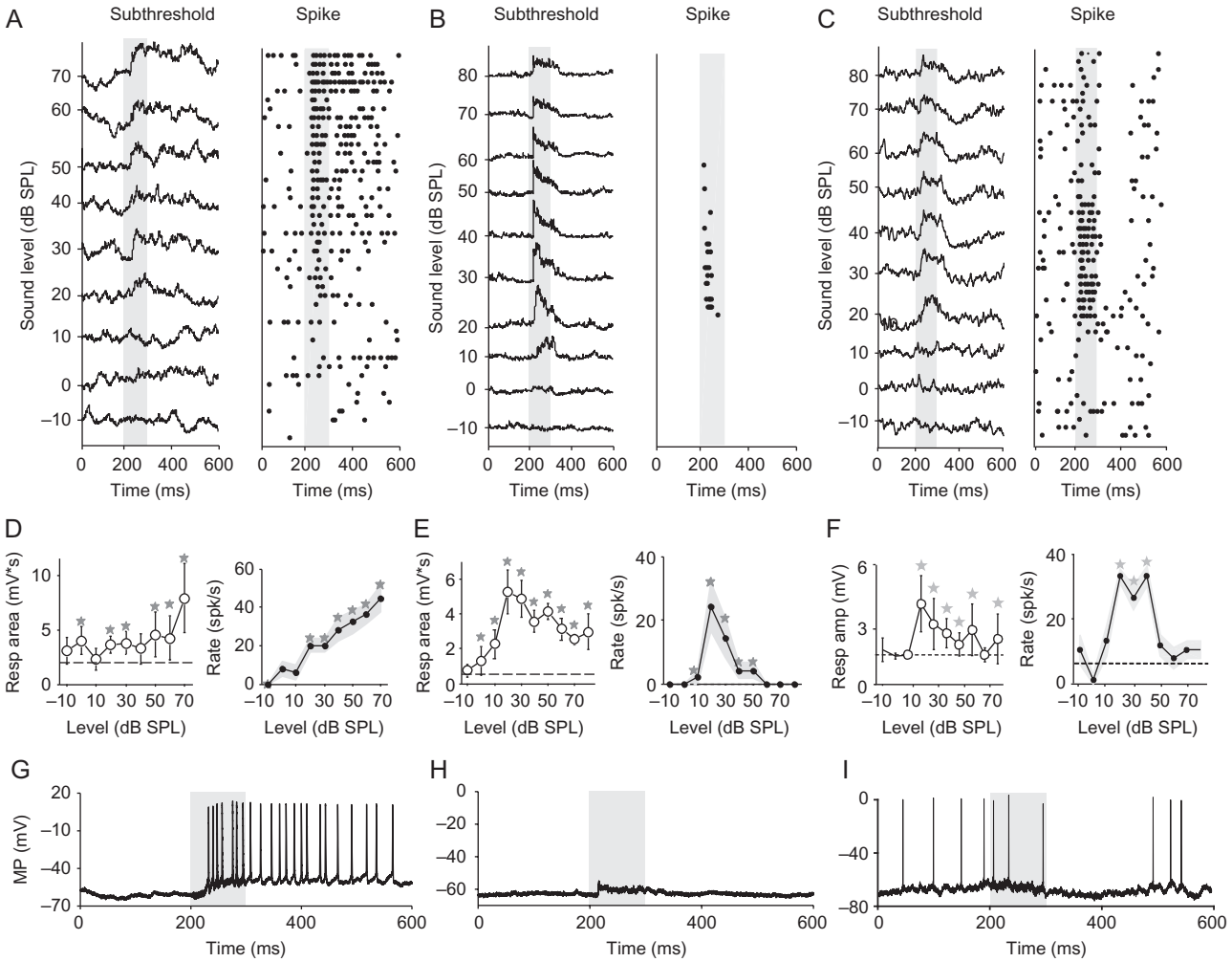

Figure 3. Rate-level functions of subthreshold and spiking responses of A1 neurons. *A*, Subthreshold (left) and spiking (right) responses of a representative A1 neuron (M22W1828) with monotonic rate-level function in response to BF tone with varying sound level. The spike width is 0.69 ms. Gray shaded area indicates the time periods of pure tone stimuli. *B*, *C*, Subthreshold (left) and spiking (right) responses of 2 representative A1 neurons (M22W0295, M22W0259) with non-monotonic rate-level functions. The spike width is 0.31 and 0.29 ms, respectively. *D*, *E*, *F*, Subthreshold response magnitude (left) and firing rate (right) averaged over the duration of the pure tone stimuli and across 5 trials plotted against the sound level, for the three example neurons shown in *A*–*C*, respectively. Error bars and gray area show standard deviations. Dashed horizontal lines indicate mean spontaneous subthreshold response (left) and mean spontaneous firing rate (right) of each neuron. Asterisks indicate that evoked responses are significantly different from spontaneous responses. *G*, *H*, *I*, Example recording traces of response to BF tone at the loudest sound level tested for the three example neurons in *A*–*C*, respectively. Gray shaded area indicates the duration of pure tone stimuli.

inherited from thalamic inputs, but created in the transformation from subthreshold to spiking response at the level of individual A1 neurons.

Frequency and Intensity Selectivity of Regular-spiking and Fast-spiking Neurons

The interplay between excitatory and inhibitory synaptic inputs determines cortical neurons' responses to sound features. Intracortical inhibition provided by local GABAergic interneurons is known to play an essential role for sound processing (Wu et al. 2006, 2008; Sadagopan and Wang 2010; Haider et al. 2013). Identifying response properties of regular-spiking (RS) and fast-spiking (FS) neurons in awake animals is critical to understand their contributions in cortical circuits (Hangya et al. 2014; Li et al. 2014, 2015). Sharp electrode recordings used in the present study allowed us to record from both large pyramidal neurons and small-sized interneurons. We were able to collect stable spike waveform data from 89 of 106 intracellularly recorded A1 neurons to perform the shape analysis. These neurons were classified into RS and FS neurons by their spike shapes base on the method established in previous studies (McCormick et al. 1985; Steriade et al. 2001; Nowak et al. 2003; Cardin et al. 2007; Wu et al. 2008; Subkhankulova et al. 2010; Lewis et al. 2012; Li et al. 2014). FS neurons typically exhibited narrow spike width and pronounced AHP as shown by a representative example in Figure 5A, whereas RS neurons showed broad spike width and weak AHP as shown by a representative example in Figure 5B. We separated the 89 intracellularly recorded A1 neurons into 2 clusters of 65 RS neurons and 21 FS neurons, respectively, in the space defined by spike width at half height and the slope of AHP (Fig. 5C–E). Three neurons fell outside of the 2 clusters and were excluded from further analyses.

Based on this classification scheme, we next compared FS and RS neurons in term of their frequency and intensity selectivity properties. We obtained frequency response data from 55 of 89 neurons. Supplementary Figure S2 shows frequency and

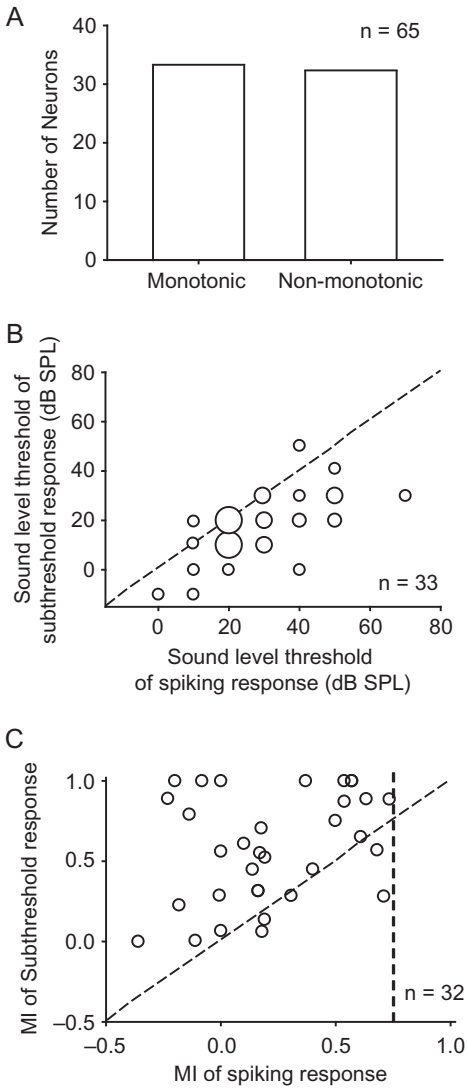

Figure 4. Quantitative analysis of monotonicity and sound level threshold. *A*, Distribution of neurons with monotonic or non-monotonic rate-level function. Neurons with the monotonicity index (MI) of firing rate (see Materials and Methods) greater than 0.75 were defined as neurons with monotonic rate-level function ($n = 33$), whereas neurons with the MI less than 0.75 were defined as neurons with non-monotonic rate-level function ($n = 32$). *B*, Sound level threshold of subthreshold response is plotted against that of spiking response for the neurons with monotonic rate-level function ($n = 33$). The size of circles is proportional to the number of neurons with the same threshold. *C*, MI of subthreshold response is plotted against that of spiking response for the neurons with non-monotonic rate-level function ($n = 32$). The vertical dashed line indicates MI of 0.75 in spiking response (see Materials and Methods).

intensity responses of 5 FS neurons. For both spiking and subthreshold responses, FS neurons showed a larger mean and a greater variation in frequency tuning bandwidth than RS neurons (Fig. 6*A*,*B*, Supplementary Fig. S1A). On average, tuning bandwidths of FS neurons for spiking and subthreshold responses were 0.64 ± 0.11 and 1.17 ± 0.24 octaves (mean ± SE, $n = 12$), respectively, which were significantly broader than those of RS neurons (spiking, 0.39 ± 0.04 octaves; subthreshold, 0.73 ± 0.09 octaves, mean ± SE, $n = 43$, $p = .02$ and 0.015, respectively, student *t*-test). We examined sound intensity responses in 65 neurons where sufficient data were obtained from 20 FS neurons and 45 RS neurons. Both FS and RS groups had monotonic and non-monotonic neurons, with a slightly higher proportion of monotonic neurons in the FS group (60%, 12/20 neurons) than in the RS group (47%, 21/45 neurons) (Fig. 6*C*–*E*, Supplementary Fig. S1B). On average, the MI of spiking response was significantly larger in FS neurons than in RS neurons (mean ± SE, spiking, FS: 0.66 ± 0.09, $n = 20$; RS: 0.52 ± 0.07, $n = 45$, P = 0.02, student *t*-test; subthreshold, FS: 0.48 ± 0.08, $n = 20$; RS: 0.37 ± 0.08, $n = 45$, P = 0.36). The above analyses indicated that RS neurons as a group showed greater frequency selectivity and were more non-monotonic than FS neurons in awake marmoset A1. We further analyzed the relationship between mean resting MP and spontaneous firing rate (see Supplementary Fig. S1C) and between spike width spontaneous firing rate (Fig. S1D). A1 neurons with low spontaneous firing rate had relatively lower resting MP and larger MP fluctuations in comparison to neurons with high spontaneous firing rate (see Supplementary Fig. S1C). There was a weak negative correlation between spike width spontaneous firing rate (see Supplementary Fig. S1D).

Discussion

The present study represents one of a few efforts to investigate subthreshold mechanisms underlying temporal diversity and stimulus feature selectivity in A1 of awake animals. Using a novel intracellular recording method developed in awake marmosets, we found that A1 neurons sharpened frequency tuning and enhanced non-monotonicity in rate-level function from subthreshold to spiking responses. Our findings provide valuable insights into cellular mechanisms underlying auditory processing in A1 of awake animals.

Subthreshold Mechanisms Underlying Sustained Firing

Previous studies have showed that cortical responses to sensory stimuli observed in awake animals differ in some important ways from those observed in anesthetized animals (Wang et al. 2005, 2008; Ter-Mikaelian et al. 2007; Constantinople and Bruno 2011; Long and Lee 2012; Haider et al. 2013; Gao and Wehr 2015; Gao et al. 2016). Neurons in the auditory cortex of awake animals exhibited both sustained and transient spiking responses to acoustic stimulation (Bieser and Muller-Preuss 1996; Recanzone 2000; Wang et al. 2005; Qin et al. 2008; Gao and Wehr 2015; McGinley et al. 2015; Gao et al. 2016). Studies in awake marmosets showed that the temporal response patterns of A1 neurons changed dynamically with sound parameters, in such a way that sustained responses were more likely observed at a neuron's preferred stimuli (Wang et al. 2005, 2008). This suggests that onset responses are driven by inputs that are less selective than those that give rise to sustained responses.

Our intracellular recording results revealed that A1 neurons of awake marmosets exhibited diverse temporal response patterns in subthreshold responses when the parameters of sound stimuli varied. In general, sustained firing is closely correlated with sustained depolarization and onset firing is closely correlated with transient depolarization. Based on our observations, we propose potential synaptic mechanisms underlying sustained firing. A1 neurons' membrane potentials typically fluctuate spontaneously below the spiking threshold without auditory inputs. When preferred stimuli are presented, A1 neurons receive a large number of persistent synaptic inputs from the thalamus or other cortical sources, which give rise to sustained depolarization to reach spike threshold. As a result,

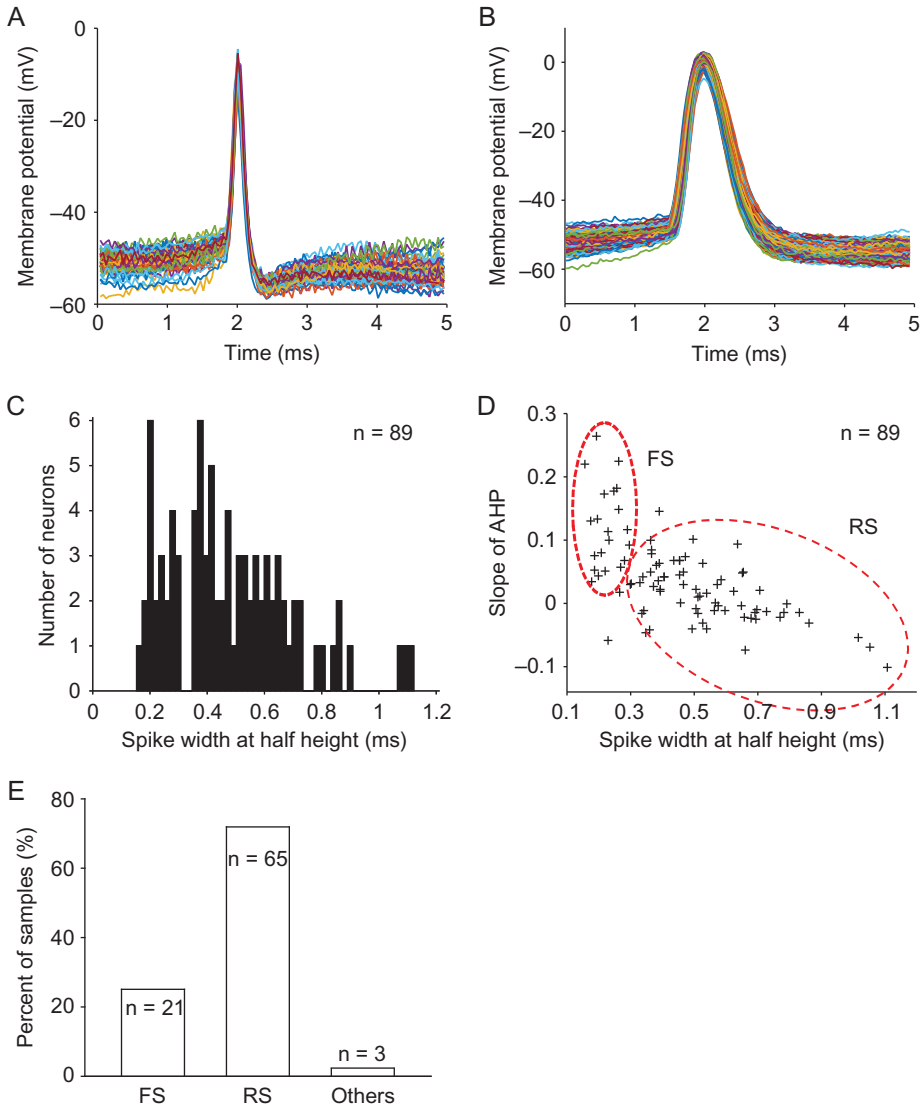

Figure 5. Classification of regular-spiking (RS) and fast-spiking (FS) neurons. *A*, *B*, Overlay of action potentials from 2 representative A1 neurons (M22W1522, M14U1076) with narrow (*A*) and broad (*B*) spike waveforms, respectively. *C*, Distribution of spike width (at half-amplitude, see Materials and Methods) of 89 A1 neurons with stable spike waveform. *D*, Slope of after-hyperpolarization-potential (AHP) (see Materials and Methods) is plotted against the spike width of 89 A1 neurons. The neurons are separated into RS and FS populations as indicated by 2 red ellipses. *E*, Number of classified RS and FS neurons. "Others" indicates neurons that were excluded from the 2 types.

sustained spiking activity is generated throughout the period of sustained depolarization. However, in contrast to the observations from awake marmosets, previous studies in A1 of awake rats reported limited sustained firing or sustained depolarization (Hromadka et al. 2013) to sound stimulation. These discrepancies could be due to differences in species or methodology as cortical neurons can be highly selective, showing only sustained responses for a specific combinations of spectral, temporal, and intensity parameters (Wang et al. 2005). A few studies showed that intracortical excitatory inputs modulated sustained rather than onset responses of cortical neurons (Li et al. 2013; Lien and Scanziani 2013). Transient responses were predominant in anesthetized animals, which could be explained by the lack of the intracortical excitatory inputs which are suppressed under anesthesia. The differences of cortical processing between anesthetized and awake states may also be due to the top-down influences by the animals' internal brain states (Gilbert and Sigman 2007; Duarte 2015; McGinley et al. 2015; Lorincz and Adamantidis 2016).

Transformations from Subthreshold to Spiking Responses in Frequency and Intensity Selectivity

Our study revealed the refinement in frequency selectivity from subthreshold to spiking responses, which provides direct evidence of the transformation in frequency domain that takes place at the level of individual A1 neurons in the awake condition. Furthermore, we found an enhancement of non-monotonicity in A1 spiking responses. Non-monotonic intensity tuning is related to "O-shaped" frequency response areas (FRAs) which is more prominent in A1 of awake animals (Pfingst and O'Connor 1981; Sadagopan and Wang 2008, 2010) than anesthetized animals (Schreiner and Mendelson 1990; Sadagopan and Wang 2008). It has been suggested that "O-shaped" FRAs may lead to a

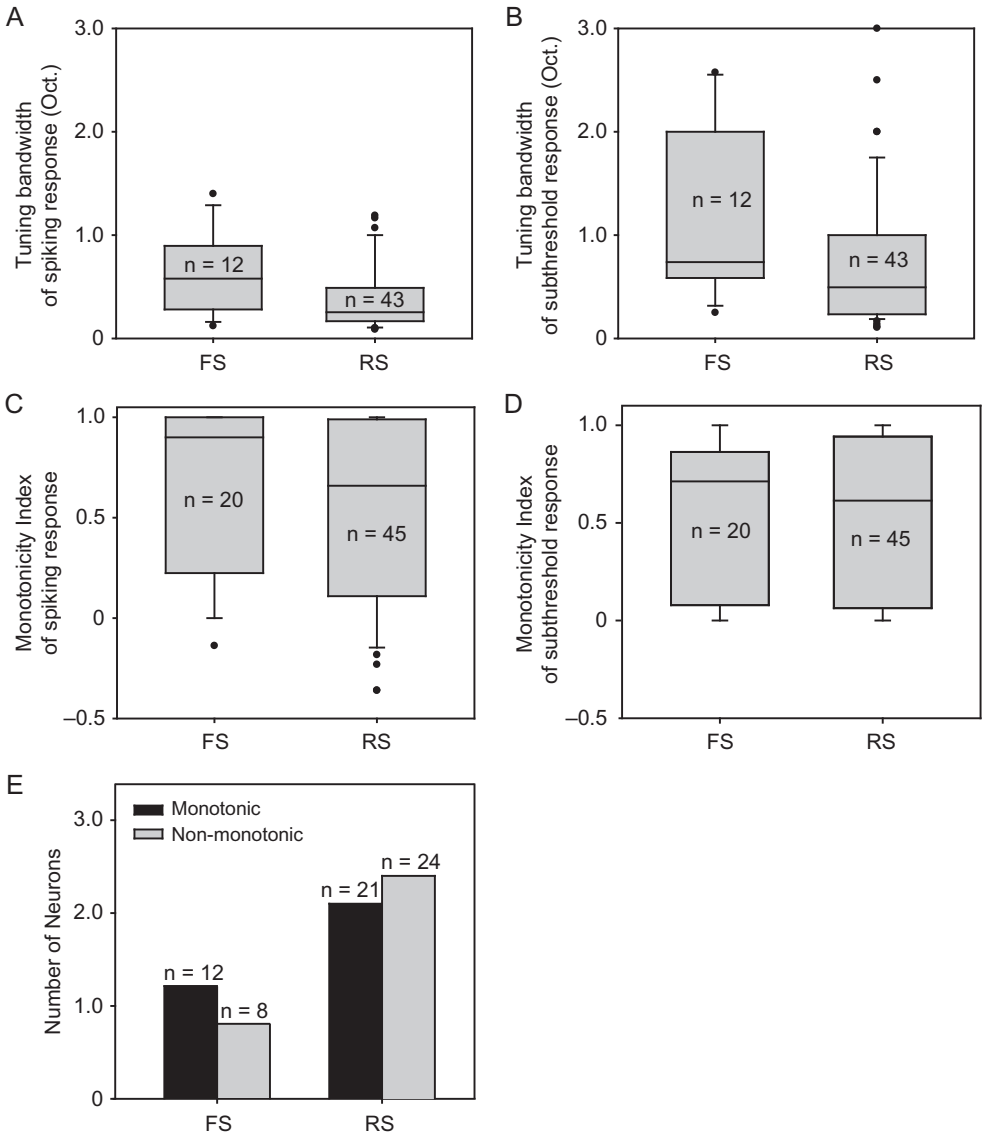

Figure 6. Comparison between FS and RS neurons. *A*, Tuning bandwidths of spiking response for FS ($n = 12$) and RS ($n = 43$) neurons. Boxes show 25th and 75th percentiles. The middle line inside the box represents the median and the whiskers indicate 95th and 5th percentiles. Data beyond the whiskers are displayed in dots. *B*, Tuning bandwidths of subthreshold response for FS ($n = 12$) and RS ($n = 43$) neurons. Format is the same as in *A*. *C–D*, MI of spiking (C) and subthreshold response (D) for FS ($n = 20$) and RS ($n = 45$) neurons, respectively. Format is the same as in *A*. *E*, Number of monotonic and non-monotonic neurons in FS ($n = 20$) and RS ($n = 45$) subpopulations, respectively.

level-invariant representation of sounds over the population of A1 neurons (Sadagopan and Wang 2008). The enhancement of non-monotonicity in awake A1 is yet another example of the transformation from thalamic inputs to cortical outputs in A1.

The auditory thalamus has been shown to be less selective to sound features than auditory cortex. Bartlett et al. (2011) showed that frequency tuning was narrower during the sustained response compared with the onset response in auditory cortex, but not in auditory thalamic (Bartlett et al. 2011). Whole cell recording study from auditory cortex of awake rats showed that the sustained response fade away when the auditory cortex was silenced by activating the local parvalbumin-expressing interneurons via opotogenetic technique (Li et al. 2013). These studies suggest that intracortical connections play an important role in shaping the sustained responses and stimulus feature selectivity in the auditory cortex of awake animals. However, further investigations are necessary to separate contributions of thalamocortical and intracortical inputs to A1 neurons.

Contributions of Intracortical Inhibition in Cortical Refinement in A1 Under Awake Condition

Previous experiments in anesthetized animals and computational modeling have provided some hints to synaptic mechanisms underlying cortical sound processing. It has been suggested that synaptic inhibition plays an essential role for producing sound feature selectivity and temporal diversity. The co-tuned network with balanced excitatory and inhibitory inputs was proposed to produce essentially transient firing, V-shaped FRAs, and monotonic rate-level functions in spiking responses (Wehr and Zador 2003; Tan et al. 2004; de la Rocha et al. 2008), whereas a lateral inhibitory network, where

frequency range with inhibitory input was broader than that of excitatory input, is able to produce a variety of response properties such as O-shaped FRAs with narrow frequency tuning and non-monotonic rate-level function (Wu et al. 2006, 2008; de la Rocha et al. 2008; Li et al. 2014). In comparison to anesthetized animals, a larger proportion of non-monotonic neurons and O-shaped FRAs were observed in A1 of awake animals, which suggests that A1 neurons in the awake state may receive stronger inhibitory inputs (Sadagopan and Wang 2010; Haider et al. 2013). However, it is extremely difficult to separate excitatory from inhibitory inputs in awake animals in order to study synaptic mechanisms and contributions by intracortical inhibition. In the present study, we attempted to identify excitatory and inhibitory neurons in A1 of awake marmosets by sharp electrode recordings. Because cell-type specific labeling techniques which are used frequently in rodents are not yet available in marmosets, the classification based on neurons' spike shapes serves as an alternative method to identify the cell-type specific cortical functions in non-human primates. The analyses of FS and RS neurons in this study (Figs 5–6, Supplementary Figs. S1–S2) represent the first effort to identify inhibitory and excitatory neurons in auditory cortex of awake marmosets.

Overall, FS neurons exhibited broader frequency tuning properties with more monotonic intensity tuning neurons than RS neurons. FS neurons with broader frequency tuning may provide feedforward lateral inhibition to excitatory neurons, which helps sharpen the cortical selectivity in frequency tuning. Our results were consistent with the results obtained from parvalbumin-positive (PV) expressing neurons obtained from transgenic mice which were characterized as FS neurons by their electrophysiological properties (Li et al. 2015). The broader frequency tuning in FS neurons as compared with RS neurons observed in awake marmoset A1 supports the hypothesis of lateral inhibitory network in A1. The larger proportion of monotonic FS neurons than RS neurons in A1 supports the hypothesis that non-monotonicity was generated by the interplay between monotonic inhibitory inputs and non-monotonic excitatory inputs. However, the sharp electrode recording has limitations in that we cannot separate excitatory form inhibitory inputs in individual cortical neurons and thus we cannot unmask the synaptic mechanisms underlying sound processing in awake animals with this technique. New techniques, such as optogenetic manipulations may be combined with sharp electrode recordings to improve our understanding of these questions.

Supplementary Material

Supplementary material is available at *Cerebral Cortex* online.

Funding

This work was supported by National Institutes of Health Grant DC003180 (X.W.).

Notes

We thank Yunyan Wang at Johns Hopkins University for providing some intracellular recording data for population analyses, Xinjian Li at National Institutes of Health for writing the Matlab analysis programs and discussing and analyzing the data, and Shiyong Huang, Kaiwen He, and Alfredo Kirkwood at Johns Hopkins University for providing access and technical support for the laser-based pipette puller. *Conflict of Interest*: The authors declare no competing financial interests.

References

Agamaite JA, Chang C-J, Osmanski MS, Wang X. 2015. A quantitative acoustic analysis of the vocal repertoire of the common marmoset (Callithrix jacchus). J Acoust Soc Am. 138:2906–2928.

Bartlett EL, Sadagopan S, Wang X. 2011. Fine frequency tuning in monkey auditory cortex and thalamus. J Neurophysiol. 106:849–859.

Bendor D, Wang X. 2007. Differential neural coding of acoustic flutter within primate auditory cortex. Nat Neurosci. 10:763–771.

Bendor D, Wang X. 2008. Neural response properties of primary, rostral, and rostrotemporal core fields in the auditory cortex of marmoset monkeys. J Neurophysiol. 100:888–906.

Bieser A, Muller-Preuss P. 1996. Auditory responsive cortex in the squirrel monkey: neural responses to amplitude-modulated sounds. Exp Brain Res. 108:273–284.

Brugge JF, Merzenich MM. 1973. Responses of neurons in auditory cortex of the macaque monkey to monaural and binaural stimulation. J Neurophysiol. 36:1138–1158.

Cardin JA, Palmer LA, Contreras D. 2007. Stimulus feature selectivity in excitatory and inhibitory neurons in primary visual cortex. J Neurosci. 27:10333–10344.

Chambers AR, Hancock KE, Sen K, Polley DB. 2014. Online stimulus optimization rapidly reveals multidimensional selectivity in auditory cortical neurons. J Neurosci. 34(27):8963–8975.

Constantinople CM, Bruno RM. 2011. Effects and mechanisms of wakefulness on local cortical networks. Neuron. 69:1061–1068.

de la Rocha J, Marchetti C, Schiff M, Reyes AD. 2008. Linking the response properties of cells in auditory cortex with network architecture: cotuning versus lateral inhibition. J Neurosci. 28:9151–9163.

DeWeese MR, Wehr M, Zador AM. 2003. Binary spiking in auditory cortex. J Neurosci. 23:7940–7949.

Duarte R. 2015. Expansion and state-dependent variability along sensory processing streams. J Neurosci. 35:7315–7316.

Fritz JB, David SV, Radtke-Schuller S, Yin P, Shamma SA. 2010. Adaptive, behaviorally gated, persistent encoding of task-relevant auditory information in ferret frontal cortex. Nat Neurosci. 13:1011–1019.

Fritz JB, Elhilali M, Shamma SA. 2007. Adaptive changes in cortical receptive fields induced by attention to complex sounds. J Neurophysiol. 98:2337–2346.

Gao L, Kostlan K, Wang Y, Wang X. 2016. Distinct subthreshold mechanisms underlying rate-coding principles in primate auditory cortex. Neuron. 91:905–919.

Gao X, Wehr M. 2015. A coding transformation for temporally structured sounds within auditory cortical neurons. Neuron. 86:292–303.

Gilbert CD, Sigman M. 2007. Brain states: top-down influences in sensory processing. Neuron. 54:677–696.

Haider B, Hausser M, Carandini M. 2013. Inhibition dominates sensory responses in the awake cortex. Nature. 493:97–100.

Hangya B, Pi HJ, Kvitsiani D, Ranade SP, Kepecs A. 2014. From circuit motifs to computations: mapping the behavioral repertoire of cortical interneurons. Curr Opin Neurobiol. 26:117–124.

Heil P. 1997. Auditory cortical onset responses revisited. II. Response strength. J Neurophysiol. 77:2642–2660.

Hromadka T, Deweese MR, Zador AM. 2008. Sparse representation of sounds in the unanesthetized auditory cortex. PLoS Biol. 6:e16.

Hromadka T, Zador AM, DeWeese MR. 2013. Up states are rare in awake auditory cortex. J Neurophysiol. 109:1989–1995.

Issa EB, Wang X. 2008. Sensory responses during sleep in primate primary and secondary auditory cortex. J Neurosci. 28: 14467–14480.

Kajikawa Y, de La Mothe L, Blumell S, Hackett TA. 2005. A comparison of neuron response properties in areas A1 and CM of the marmoset monkey auditory cortex: tones and broadband noise. J Neurophysiol. 93:22–34.

Kitano K, Cateau H, Kaneda K, Nambu A, Takada M, Fukai T. 2002. Two-state membrane potential transitions of striatal spiny neurons as evidenced by numerical simulations and electrophysiological recordings in awake monkeys. J Neurosci. 22:RC230.

Lee AK, Epsztein J, Brecht M. 2009. Head-anchored whole-cell recordings in freely moving rats. Nat Protoc. 4:385–392.

Lee AK, Epsztein J, Brecht M. 2014a. Whole-cell patch-clamp recordings in freely moving animals. Methods Mol Biol. 1183:263–276.

Lee AK, Manns ID, Sakmann B, Brecht M. 2006. Whole-cell recordings in freely moving rats. Neuron. 51:399–407.

Lee D, Shtengel G, Osborne JE, Lee AK. 2014b. Anesthetized- and awake-patched whole-cell recordings in freely moving rats using UV-cured collar-based electrode stabilization. Nat Protoc. 9:2784–2795.

Lewis LD, Weiner VS, Mukamel EA, Donoghue JA, Eskandar EN, Madsen JR, Anderson WS, Hochberg LR, Cash SS, Brown EN, et al. 2012. Rapid fragmentation of neuronal networks at the onset of propofol-induced unconsciousness. Proc Natl Acad Sci U S A. 109:E3377–E3386.

Li LY, Ji XY, Liang F, Li YT, Xiao Z, Tao HW, Zhang LI. 2014. A feedforward inhibitory circuit mediates lateral refinement of sensory representation in upper layer 2/3 of mouse primary auditory cortex. J Neurosci. 34:13670–13683.

Li LY, Li YT, Zhou M, Tao HW, Zhang LI. 2013. Intracortical multiplication of thalamocortical signals in mouse auditory cortex. Nat Neurosci. 16:1179–1181.

Li LY, Xiong XR, Ibrahim LA, Yuan W, Tao HW, Zhang LI. 2015. Differential receptive field properties of parvalbumin and somatostatin inhibitory neurons in mouse auditory cortex. Cereb Cortex. 25:1782–1791.

Liang L, Lu T, Wang X. 2002. Neural representations of sinusoidal amplitude and frequency modulations in the primary auditory cortex of awake primates. J Neurophysiol. 87: 2237–2261.

Lien AD, Scanziani M. 2013. Tuned thalamic excitation is amplified by visual cortical circuits. Nat Neurosci. 16:1315–1323.

Long MA, Jin DZ, Fee MS. 2010. Support for a synaptic chain model of neuronal sequence generation. Nature. 468:394–399.

Long MA, Lee AK. 2012. Intracellular recording in behaving animals. Curr Opin Neurobiol. 22:34–44.

Lorincz ML, Adamantidis AR. 2016. Monoaminergic control of brain states and sensory processing: existing knowledge and recent insights obtained with optogenetics. Prog Neurobiol. 151:237–253.

Lu T, Liang L, Wang X. 2001a. Neural representations of temporally asymmetric stimuli in the auditory cortex of awake primates. J Neurophysiol. 85:2364–2380.

Lu T, Liang L, Wang X. 2001b. Temporal and rate representations of time-varying signals in the auditory cortex of awake primates. Nat Neurosci. 4:1131–1138.

Lu T, Wang X. 2000. Temporal discharge patterns evoked by rapid sequences of wide- and narrowband clicks in the primary auditory cortex of cat. J Neurophysiol. 84:236–246.

Malone BJ, Scott BH, Semple MN. 2002. Context-dependent adaptive coding of interaural phase disparity in the auditory cortex of awake macaques. J Neurosci. 22:4625–4638.

Matsumura M, Cope T, Fetz EE. 1988. Sustained excitatory synaptic input to motor cortex neurons in awake animals revealed by intracellular recording of membrane potentials. Exp Brain Res. 70:463–469.

McCormick DA, Connors BW, Lighthall JW, Prince DA. 1985. Comparative electrophysiology of pyramidal and sparsely spiny stellate neurons of the neocortex. J Neurophysiol. 54:782–806.

McGinley MJ, David SV, McCormick DA. 2015a. Cortical membrane potential signature of optimal states for sensory signal detection. Neuron. 87:179–192.

McGinley MJ, Vinck M, Reimer J, Batista-Brito R, Zagha E, Cadwell CR, Tolias AS, Cardin JA, McCormick DA. 2015b. Waking state: rapid variations modulate neural and behavioral responses. Neuron. 87:1143–1161.

Mesik L, Ma WP, Li LY, Ibrahim LA, Huang ZJ, Zhang LI, Tao HW. 2015. Functional response properties of VIP-expressing inhibitory neurons in mouse visual and auditory cortex. Front Neural Circuits. 9:22.

Miller CT, Freiwald WA, Leopold DA, Mitchell JF, Silva AC, Wang X. 2016. Marmosets: a neuroscientific model of human social behavior. Neuron. 90:219–233.

Mizrahi A, Shalev A, Nelken I. 2014. Single neuron and population coding of natural sounds in auditory cortex. Curr Opin Neurobiol. 24(1):103–110.

Nelken I. 2008. Processing of complex sounds in the auditory system. Curr Opin Neurobiol. 18(4):413–417.

Niell CM, Stryker MP. 2010. Modulation of visual responses by behavioral state in mouse visual cortex. Neuron. 65:472–479.

Nowak LG, Azouz R, Sanchez-Vives MV, Gray CM, McCormick DA. 2003. Electrophysiological classes of cat primary visual cortical neurons in vivo as revealed by quantitative analyses. J Neurophysiol. 89:1541–1566.

Ojima H, Murakami K. 2002. Intracellular characterization of suppressive responses in supragranular pyramidal neurons of cat primary auditory cortex in vivo. Cereb Cortex. 12:1079–1091.

Okun M, Naim A, Lampl I. 2010. The subthreshold relation between cortical local field potential and neuronal firing unveiled by intracellular recordings in awake rats. J Neurosci. 30:4440–4448.

Osmanski MS, Wang X. 1981. Measurement of absolute auditory thresholds in the common marmoset (*Callithrix jacchus*). Hear Res. 277:127–133.

Pfingst BE, O'Connor TA. 1981. Characteristics of neurons in auditory cortex of monkeys performing a simple auditory task. J Neurophysiol. 45:16–34.

Phillips DP. 1985. Temporal response features of cat auditory cortex neurons contributing to sensitivity to tones delivered in the presence of continuous noise. Hear Res. 19:253–268.

Phillips DP, Semple MN, Kitzes LM. 1995. Factors shaping the tone level sensitivity of single neurons in posterior field of cat auditory cortex. J Neurophysiol. 73:674–686.

Polack PO, Friedman J, Golshani P. 2013. Cellular mechanisms of brain state-dependent gain modulation in visual cortex. Nat Neurosci. 16:1331–1339.

Polley DB, Heiser MA, Blake DT, Schreiner CE, Merzenich MM. 2004. Associative learning shapes the neural code for stimulus magnitude in primary auditory cortex. Proc Natl Acad Sci U S A. 101:16351–16356.

Poulet JF, Petersen CC. 2008. Internal brain state regulates membrane potential synchrony in barrel cortex of behaving mice. Nature. 454:881–885.

Qin L, Wang JY, Sato Y. 2008. Representations of cat meows and human vowels in the primary auditory cortex of awake cats. J Neurophysiol. 99:2305–2319.

Recanzone GH. 2000. Response profiles of auditory cortical neurons to tones and noise in behaving macaque monkeys. Hear Res. 150:104–118.

Romo R, Salinas E. 2003. Flutter discrimination: neural codes, perception, memory and decision making. Nat Rev Neurosci. 4:203–218.

Sadagopan S, Wang X. 2008. Level invariant representation of sounds by populations of neurons in primary auditory cortex. J Neurosci. 28:3415–3426.

Sadagopan S, Wang X. 2010. Contribution of inhibition to stimulus selectivity in primary auditory cortex of awake primates. J Neurosci. 30:7314–7325.

Schreiner CE, Mendelson JR. 1990. Functional topography of cat primary auditory cortex: distribution of integrated excitation. J Neurophysiol. 64:1442–1459.

Schreiner CE, Mendelson JR, Sutter ML. 1992. Functional topography of cat primary auditory cortex: representation of tone intensity. Exp Brain Res. 92:105–122.

Schreiner CE, Read HL, Sutter ML. 2000. Modular organization of frequency integration in primary auditory cortex. Annu Rev Neurosci. 23:501–529.

Steriade M, Timofeev I, Grenier F. 2001. Natural waking and sleep states: a view from inside neocortical neurons. J Neurophysiol. 85:1969–1985.

Subkhankulova T, Yano K, Robinson HP, Livesey FJ. 2010. Grouping and classifying electrophysiologically-defined classes of neocortical neurons by single cell, whole-genome expression profiling. Front Mol Neurosci. 3:10.

Tan AY, Atencio CA, Polley DB, Merzenich MM, Schreiner CE. 2007. Unbalanced synaptic inhibition can create intensity-tuned auditory cortex neurons. Neuroscience. 146:449–462.

Tan AY, Chen Y, Scholl B, Seidemann E, Priebe NJ. 2014. Sensory stimulation shifts visual cortex from synchronous to asynchronous states. Nature. 509:226–229.

Tan AY, Zhang LI, Merzenich MM, Schreiner CE. 2004. Tone-evoked excitatory and inhibitory synaptic conductances of primary auditory cortex neurons. J Neurophysiol. 92:630–643.

Ter-Mikaelian M, Sanes DH, Semple MN. 2007. Transformation of temporal properties between auditory midbrain and cortex in the awake Mongolian gerbil. J Neurosci. 27:6091–6102.

Vidyasagar TR, Pei X, Volgushev M. 1996. Multiple mechanisms underlying the orientation selectivity of visual cortical neurones. Trends Neurosci. 19:272–277.

Wang X. 2000. On cortical coding of vocal communication sounds in primates. Proc Natl Acad Sci USA. 97:11843–11849.

Wang X, Lu T, Bendor D, Bartlett E. 2008. Neural coding of temporal information in auditory thalamus and cortex. Neuroscience. 154:294–303.

Wang X, Lu T, Snider RK, Liang L. 2005. Sustained firing in auditory cortex evoked by preferred stimuli. Nature. 435:341–346.

Watkins PV, Barbour DL. 2011. Rate-level responses in awake marmoset auditory cortex. Hear Res. 275(1–2):30–42.

Wehr M, Zador AM. 2003. Balanced inhibition underlies tuning and sharpens spike timing in auditory cortex. Nature. 426: 442–446.

Wu GK, Arbuckle R, Liu BH, Tao HW, Zhang LI. 2008. Lateral sharpening of cortical frequency tuning by approximately balanced inhibition. Neuron. 58:132–143.

Wu GK, Li P, Tao HW, Zhang LI. 2006. Nonmonotonic synaptic excitation and imbalanced inhibition underlying cortical intensity tuning. Neuron. 52:705–715.

Wu GK, Tao HW, Zhang LI. 2011. From elementary synaptic circuits to information processing in primary auditory cortex. Neurosci Biobehav Rev. 35:2094–2104.

Zanos TP, Mineault PJ, Pack CC. 2011. Removal of spurious correlations between spikes and local field potentials. J Neurophysiol. 105:474–486.

Zhang LI, Tan AY, Schreiner CE, Merzenich MM. 2003. Topography and synaptic shaping of direction selectivity in primary auditory cortex. Nature. 424:201–205.

Zhou M, Liang F, Xiong XR, Li L, Li H, Xiao Z, Tao HW, Zhang LI. 2014. Scaling down of balanced excitation and inhibition by active behavioral states in auditory cortex. Nat Neurosci. 17: 841–850.

Zhou Y, Liu BH, Wu GK, Kim YJ, Xiao Z, Tao HW, Zhang LI. 2010. Preceding inhibition silences layer 6 neurons in auditory cortex. Neuron. 65:706–717.